Ref. Ares(2026)10163158 - 29/10/2026

T H R I L L

TECHNOLOGY FOR HIGH-REPETITION-RATE
INTENSE LASER LABORATORIES

Deliverable Data	
Deliverable number	D4.3
Deliverable name	Report on concept for high-energy high-rep amplifier
Work Package	WP 4
Lead WP/deliverable beneficiary	GSI
Type and dissemination level	Report, public
Deliverable status	
Submitting author	Martin Metternich
Verified (WP leader)	Bernhard Zielbauer
Approved (Coordinator)	Vincent Bagnoud
Due date of deliverable	31.10.2026

Funded by the European Union

This project has received funding by the European Union's HORIZON-INFRA-2022-TECH-01 call under grant agreement number 101095207

Table of Contents

About THRILL 1
Executive summary 2
Abbreviations 3
1 Introduction and objectives 4
2 Prototype designs 6
2.1 Conventional PHELIX Main Amplifiers (PMA) 6
2.2 The First Main Amplifier Prototype (MAPv1) 7
2.3 The Hybrid Prototype (MAPv1.5) 8
2.4 The Optimized Prototype (MAPv2) 9
3 Prototype Characterization 10
3.1 Characterization Methodology 11
3.2 Nd:glass pumping efficiency 11
3.3 Thermal Recovery 14
4 Conclusion and Outlook 18
5 References 19

List of figures

Figure 1: Schematic top-view (left) and front-view (right) cross-section of the conventional PHELIX main amplifier (PMA). The diagram illustrates the laser axis (red arrow), housing (grey), silver reflectors (orange), flashlamps (black), blast shields (light blue), ceramic isolators/reflectors (white with black frames), Nd:glass slabs (purple), and cladding (cyan). 6

Figure 2: Schematic top-view (left) and front-view (right) cross-sections of the first main amplifier prototype (MAPv1). The diagrams illustrate the laser axis (red arrow), housing (grey), optical PTFE reflectors (white with black frames), flashlamps (black), glass blast shields (light blue), cooling water volume (dark blue), Nd:glass slabs (purple), and edge cladding (cyan)..... 7

Figure 3: Schematic top-view (left) and front-view (right) cross-sections of the first hybrid amplifier prototype (MAPv1.5). The diagrams illustrate the laser axis (red arrow), housing (grey), silver reflectors (orange), optical PTFE reflectors (white with black frames), flashlamps (black), glass blast shields (light blue), cooling water volume (dark blue), Nd:glass slabs (purple), and edge cladding (cyan)..... 8

Figure 4: Schematic top-view (left) and front-view (right) cross-sections of the optimized main amplifier prototype (MAPv2). The diagrams illustrate the laser axis (red arrow), housing (grey), silver reflectors (orange), optical PTFE reflectors (white with black frames), flashlamps (black), glass blast shields (light blue), cooling water volume (dark blue), Nd:glass slabs (purple), and edge cladding (cyan). . 9

Figure 5: Schematic overview of the PHELIX laser system infrastructure. The diagram illustrates the chirped pulse amplification (CPA) architecture, highlighting the dual frontends (nsFE and fsFE), the preamplifier section featuring the 19 mm rod amplifier, the main amplifier chain, and the key diagnostic sensors, including the Main Amplifier Sensor (MAS) at the exit. The original version of this figure was created by Ohland, J. B.. 10

Figure 6: Single-pass gain as a function of the capacitor charging voltage and electrical input energy (left), alongside the corresponding calculated Nd:glass pumping efficiency at a standard charging voltage of 15.5 kV (right). The markers denote the specific frontend utilized as the probe laser (nsFE or fsFE) for the conventional PMA and the MAP prototypes. Opaque markers with error bars represent mean values and their standard deviations, whereas semi-transparent markers denote single-shot measurements. 12

Figure 7: Strehl ratio evolution comparing several shots of the MAPv1.5 prototype to a single shot of the conventional PHELIX main amplifier (PMA4). The plot highlights the rapid recovery of MAPv1.5, the massive thermal bottleneck of PMA4, the sharp initial defocus caused by the preamplifier (PA19 only, dashed line), and a slight baseline drift in the Strehl ratio. 14

Figure 8: Strehl ratio measurements during continuous shot series for MAPv1.5 at 10-minute (top) and 5-minute (bottom) intervals. Higher repetition rates lead to a deeper cumulative Strehl drop, which is dominated by low-order aberrations as defocus and astigmatism. 15

Figure 9: Thermal recovery profiles of MAPv1.5 under varying cooling parameters, including different water flow rates and cladding cooling settings. The nearly identical curves demonstrate no significant dependency on exact flow adjustments, with lower flow rates performing comparably well or slightly better. 16

Figure 10: Comparison of the Strehl ratio recovery during a 15-minute shot series for MAPv1.5 and MAPv2, showing comparable thermal stabilization capabilities. 17

Figure 11: Focal spot profiles recorded during a MAPv2 shot series (lower measurement from Figure 10) using the nsFE probe laser, demonstrating stable spatial beam quality. 17

Disclaimer

This document is part of the deliverables from the project THRILL, which has received funding from the European Union. Views and opinions expressed are however those of the author(s) only and do not necessarily reflect those of the European Union or the European Commission. Neither the European Union nor the granting authority can be held responsible for them.

About THRILL

The THRILL project deals with providing new schemes and devices for pushing forward the limits of research infrastructures (RI) of European relevance and ESFRI landmarks. To do so, the project partners have identified several technical bottlenecks in high-energy high-repetition-rate laser technology that prevent it from reaching the technical readiness level required to technically specify and build the needed devices, and guaranteeing sustainable and reliable operation of such laser beamlines at the partnering RIs. Advancing the technical readiness of these topics is strategically aligned with the long-term plans and evolution of the ESFRI landmarks FAIR, ELI (-BL) and Eu-XFEL, and RI APOLLON, bringing them to the next level of development and strengthening their leading position.

The project is focused and deliberately restricted to three enabling technologies, which require the most urgent efforts and timely attention by the community: high-energy high-repetition-rate amplification, high-energy beam transport and optical coating resilience for large optics. To reach our goals, the major activity within THRILL will be organized around producing several prototypes demonstrating a high level of technical readiness. Our proposal is addressing not yet explored technical bottlenecks - such as transport over long distances of large-aperture laser beams via relay imaging using all-reflective optics - and aims at proposing concrete steps to increase the performances and effectiveness of the industrial community through the co-development of advanced technologies up to prototyping in operational environments.

The project is not only pushing technology, it is also offering an outstanding opportunity to train a qualified work force for RIs and industry. With this in mind, the structure of THRILL promotes synergetic work, fast transfer to industry and integrated research activities at the European level. Access to the RIs will be granted as in-kind contribution.

Executive summary

In the WP4.3 of the European project THRILL, actively-cooled large-aperture amplifier concepts were explored by developing and testing water-cooled housings and slab cooling methods compatible with the PHELIX high-energy laser at GSI. The strategy was based on a modification of the 31.5-cm-disk amplifier currently used at PHELIX, which enabled the use of spare Nd:glass slabs for the project as well as the existing pulsed power system. In addition, the prototype has the advantage that it can be rapidly fitted into the main laser system after this R&D phase.

A first version of the main amplifier prototype (MAPv1) integrated flashlamps directly into water-filled side panels. While this design successfully reduced the thermal recovery time from 90 minutes to between 5 and 10 minutes, it suffered an almost 30% drop in Nd:glass pumping efficiency. This efficiency loss was primarily caused by light absorption and the trapping of radiation within the water-filled panel. To recover this lost efficiency, two new prototypes, MAPv1.5 and MAPv2, were developed with optimized geometries. Both new designs featured slab holders embedded in the reflector surface to eliminate free space between the slabs and the top and bottom panels, alongside spectral silver reflectors instead of diffuse reflectors to direct the radiation from the flashlamps toward the Nd:glass slabs. In MAPv2, the flashlamps were placed beside the water panels instead of inside them. Consequently, the water acted purely as thermal isolation for the interior and did not directly cool the flashlamps. This structural change prevented flash light radiation from being trapped by total internal reflection at steep angles and significantly reduced the path length of the light rays through the water, minimizing the absorption of infrared pump light. The hybrid prototype, MAPv1.5, incorporated most of the geometric and reflector improvements of MAPv2 but kept the flashlamps submerged inside the water panels.

Performance comparisons show that these structural changes successfully restored the lost efficiency. MAPv2 matched the pumping efficiency of the conventional PHELIX amplifiers, outperforming the hybrid MAPv1.5. Regarding the long-term aberration recovery time, the comparison between the prototypes is inherently challenging, since it is difficult to isolate amplifier-specific thermal effects from general ambient drift. Crucially, single-shot optical performance remains almost identical across all setups. Deviations only emerge during intensive shot series with shot rates of 5-10 minutes. Yet, even under these demanding conditions, mainly low-order aberrations such as defocus and astigmatism accumulate, which can most likely be compensated by adaptive optics in the future. Thus, MAPv2 provides a highly successful design, resolving the initial efficiency loss while continuing to vastly outperform traditional nitrogen-flushed systems in thermal recovery.

Abbreviations

Abbreviation	Definition
THRILL	Technology for High-Repetition Rate Intense Laser Laboratories
GSI	GSI Helmholtzzentrum für Schwerionenforschung GmbH
PHELIX	Petawatt Hoch-Energie Laser für SchwerIoneneXperimente
HEHRR	High-energy, high-repetition-rate
Nd	Neodym
CPA	Chirped Pulse Amplification
cw	Continuous wave
PTFE	Polytetrafluorethylen
PMA	PHELIX main amplifier
MAPv1	The first main amplifier prototype
MAPv1.5	The hybrid main amplifier prototype
MAPv2	The optimized main amplifier prototype
ASE	Amplified spontaneous emission
nsFE	Nanosecond frontend of PHELIX
fsFE	Femtosecond frontend of PHELIX
MAS	Main amplifier sensor of PHELIX
PA19	19 mm rod amplifier of the PHELIX preamplifier system

1 Introduction and objectives

High-energy, high-repetition-rate (HEHRR) laser systems remain scarce because they require large optical components, which are challenging to stabilize thermally. For this reason, as part of Work Package 4 (WP4.3) of the European THRILL project, we have explored alternative large-aperture amplifier concepts. Our investigations focused on two critical areas: the thermal isolation of the amplifier's interior and the active cooling of the Nd:glass slabs and their surroundings.

The development strategy within THRILL work package 4.3 followed a staged approach, compartmentalizing different functional aspects of the laser amplifier design. This seemed to be the most rational approach to a system with a complex interplay between optical, thermal and mechanical effects which can be seen as a typical multiphysics problem. Furthermore, a change in the optical part, i.e., the laser glass slabs was seen as the most problematic because of the highly sensitive but currently very hard to replace Nd:glass material. Since many physical properties of the system, like the local bulk temperature of the different amplifier components or the mechanical stress present in the laser glass are very hard to access directly, a full experimental characterization or complete simulation model were beyond the scope of the project. Thus, for the first part of the work package, the handling of the pumping process and optimization of the pump cavity were treated independently from actively cooling the laser glass slabs themselves. For this part, the slabs were seen as passive elements under the influence of the pump light and their environmental conditions.

To this end, three water-cooled prototype housings were tested in the main amplifier chain of the PHELIX high-power laser at GSI over the last four years. This provided a direct comparison to the conventional nitrogen-flushed main amplifiers typically operated in the PHELIX system. In parallel, two approaches to actively cooling the slabs themselves were investigated, but due to the challenges encountered therein and the high success of the approach of cooling everything but the slabs, these considerations will not feature in the currently proposed amplifier design. Further details will be given in annex **Fehler! Verweisquelle konnte nicht gefunden werden.**.

The first Main Amplifier Prototype (MAPv1), tested in 2024, consisted of four water-filled panels with flashlamps integrated directly into the water volume of the side panels. This design reduced the recovery time from long-term aberrations after optical pumping from 90 minutes to just 5–10 minutes compared to conventional nitrogen-flushed systems. However, this came at the cost of an almost 30% lower Nd:glass pumping efficiency. These initial findings have been published in a conference proceeding (Metternich, M, et al., 2025).

For the subsequent prototypes (MAPv1.5 and MAPv2), the primary objective was to increase the

Nd:glass pumping efficiency while maintaining, or further improving, the 5- to 10-minute aberration recovery time. In the first of the following chapters, the designs of all three prototypes are detailed. The subsequent chapters present and discuss the characterization measurements, focusing first on the Nd:glass pumping efficiency and finally on the recovery of long-term aberrations.

In the second part of WP 4.3, different ideas of actively handling the thermal load within the glass slabs were investigated. The ATON laser system under scrutiny in WP 4.1 is already very successfully featuring such an approach in its daily operation, as is outlined in deliverable D4.1. However, the insight and experience gathered there also revealed the challenges of this design based on full immersion of the laser glass slabs in a colling liquid which then becomes part of the laser light's optical path. Apart from the fact that currently, the technology involved in the ATON system is not commercially available anymore, the effort to mitigate the effects of partially liquid optical elements is considerable and does not scale well to larger beam apertures. With this in mind, two different approaches to actively cooling the laser glass were investigated. First, a simplified laser glass module design with a single layer of liquid sandwiched between two Nd:glass discs was investigated for its viability. Since the hydraulic, mechanical and optical problems involving such a setup were found to be highly challenging, this strategy was changed to using a stream of temperature-controlled air in-between the laser glass discs, which to present seems the more viable approach.

The availability of the PHELIX main amplifier system was strongly limited due to the facility's operation schedule. Since this was the only viable way to investigate an amplifier design both with flashlamp pumping and with the high-resolution wavefront measurement system which is part of the PHELIX diagnostics suite, priority was given to tests with the MAP designs described above because the probability of a high impact on the amplifier performance was deemed higher with this approach. As a consequence, all glass module tests were carried out in part either with only localized temperature measurements or on a full-aperture optical test bench with more readily available heat sources, simulating a thermal loading similar to the flash lamps in terms of energy absorbed in the laser glass during the pumping process. Both approaches were accompanied by thermodynamic simulations carried out in ANSYS, but due to the complex interplay on the solid/liquid/glass interfaces, this so far did not yield a considerable advantage. More details can be found on the report on THRILL milestone M13 which had the goal of testing a glass module prototype in a full main amplifier head.

In view of the results achieved with the MAPs, this was proven to be the correct choice for considerably increasing the repetition rate of a single amplifier head from more than 90 minutes by more than a factor of 10. For experimental campaigns carried out at a PHELIX system upgraded

with this design or future high-energy systems, has an immense value.

2 Prototype designs

This chapter details the structural and geometrical designs of the conventional PHELIX main amplifiers and the three water-cooled prototypes. Because the physical arrangement of the flashlamps, water panels, and reflectors directly governs the thermal isolation capabilities and the Nd:glass pumping efficiency, a thorough understanding of these setups is essential for interpreting the subsequent performance evaluations. Section 2.1 introduces the conventional nitrogen-flushed PHELIX amplifier, which serves as the standard reference point for all performance comparisons. Section 2.2 details the initial baseline design of the first water-cooled prototype, MAPv1. Following this, Section 2.3 describes the structural modifications implemented in the intermediate hybrid prototype, MAPv1.5. Finally, Section 2.4 presents the fully optimized geometry of MAPv2.

2.1 Conventional PHELIX Main Amplifiers (PMA)

Figure 1 provides a schematic overview of the conventional PHELIX main amplifier (PMA), which features a clear aperture of 315 mm.

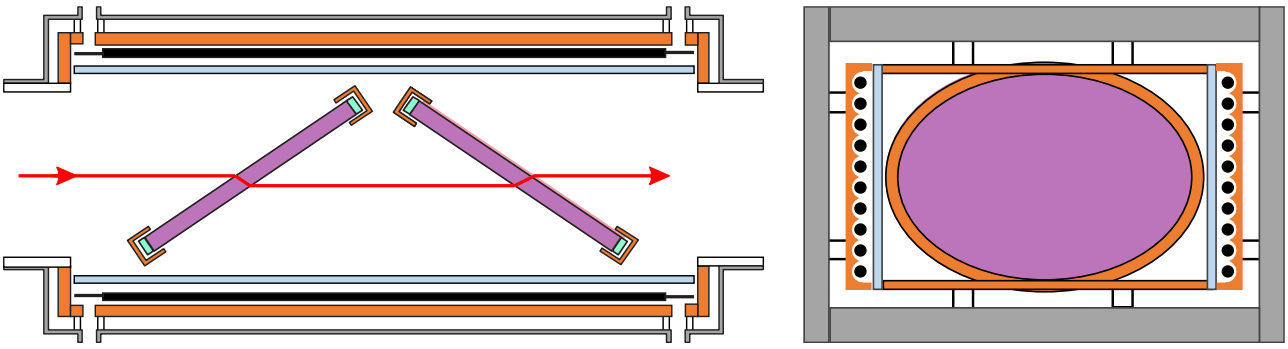


Figure 1: Schematic top-view (left) and front-view (right) cross-section of the conventional PHELIX main amplifier (PMA). The diagram illustrates the laser axis (red arrow), housing (grey), silver reflectors (orange), flashlamps (black), blast shields (light blue), ceramic isolators/reflectors (white with black frames), Nd:glass slabs (purple), and cladding (cyan).

The gain medium consists of two large-aperture Nd:glass slabs (octagonal Schott LG-750 Nd:glass with dimensions of approximately 635 mm × 340 mm × 43 mm) arranged in a Brewster angle configuration. Due to the substantial dimensions of these slabs, amplified spontaneous emission (ASE) and parasitic transverse lasing are significant limiting factors. To prevent trapped modes (caused by total internal reflection at the slab boundaries) from depleting the stored population inversion, the perimeter of each slab is equipped with an index-matched, highly absorbing edge

cladding. The amplifier is optically pumped by 20 flashlamps, each with a bore diameter of 15 mm and a length of 1120 mm. They are symmetrically distributed with 10 on each side. These are enclosed within a cavity of flat and curved silver reflectors designed to reflect the pump radiation onto the slabs. The reflector cavity is mechanically decoupled from the main housing via ceramic mounts to mitigate direct thermal conduction. Furthermore, glass blast shields are installed between the flashlamp arrays and the central amplifier cavity to protect the delicate Nd:glass slabs from acoustic shock or debris in the event of a catastrophic flashlamp failure.

Electrically, the flashlamps are driven in serially connected pairs, with each pair discharged from a bank of three parallel capacitors (C = 52 µF each) via an ignitron switch. At the default charging voltage of 15.5 kV, combined with an inductance of 650 µH, the typical discharge pulse length is 1 ms. This configuration yields an electrical pump energy of almost 10 kJ per flashlamp, amounting to a total pump energy of nearly 200 kJ for the entire amplifier module. Operating at this specific energy level corresponds to a conservative explosion fraction of 15 %. These highly moderate operating conditions ensure exceptional component longevity; historically, flashlamps in this system have endured over 20,000 shots across a 17-year timespan without any significant degradation in performance. Driven by these standard electrical parameters, the amplifier achieves a single-pass small-signal gain of 1.51(2) for a narrowband pulse at a central wavelength of 1054 nm, translating to an overall Nd:glass pumping efficiency of 1.52(5) %.

2.2 The First Main Amplifier Prototype (MAPv1)

All three water-cooled prototypes (MAPv1, MAPv1.5, and MAPv2) were specifically designed to be fully compatible with the existing PHELIX main amplifier infrastructure. By retaining the identical clear aperture, Nd:glass slabs, and flashlamp arrays, these designs facilitate a straightforward, modular upgrade of the current amplifier section. The structural baseline, MAPv1, is illustrated in Figure 2.

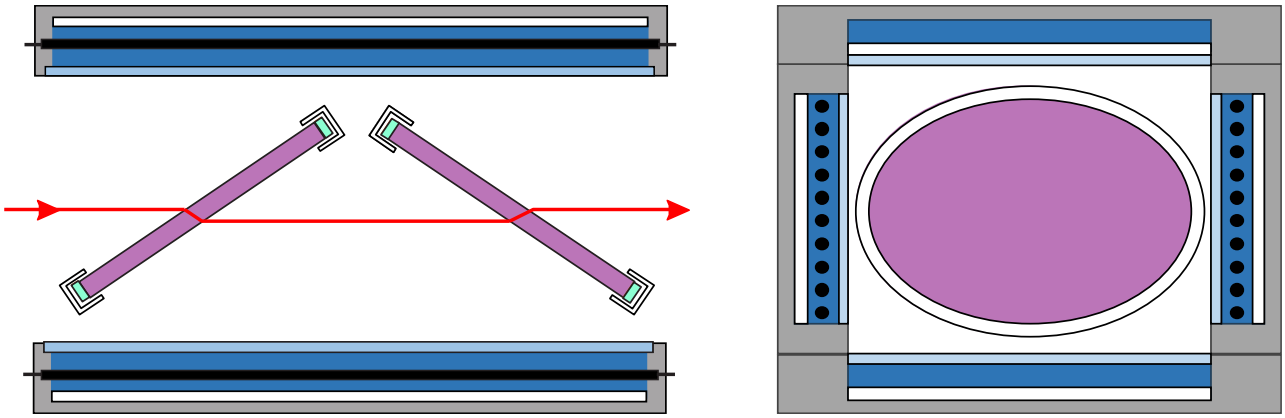


Figure 2: Schematic top-view (left) and front-view (right) cross-sections of the first main amplifier prototype (MAPv1). The diagrams illustrate the laser axis (red arrow), housing (grey), optical PTFE reflectors (white with

black frames), flashlamps (black), glass blast shields (light blue), cooling water volume (dark blue), Nd:glass slabs (purple), and edge cladding (cyan).

The assembly consists of four rectangular housing frames, each enclosed by B270 glass window plates (1100 mm × 350 mm × 10 mm). When fully assembled, the central optical cavity has combined internal dimensions of 400 mm × 400 mm × 1100 mm. This provides sufficient spatial clearance to accommodate the two large Nd:glass slabs in their standard Brewster angle configuration. The defining feature of MAPv1 is its active liquid cooling approach of all surfaces facing the laser glass slabs. Each of the four frames is hermetically sealed, allowing their internal volumes to be independently flooded with water. In this initial design, the flashlamps are directly integrated within the water volume of the two side panels. To direct the pump radiation toward the gain medium, highly reflective optical PTFE foil (Optopolymer®, manufactured by Berghof Fluoroplastic Technology GmbH) is utilized as a diffuse reflector. This foil is submerged inside all four water-filled panels and is additionally applied directly to the Nd:glass slab holders to maximize Nd:glass pumping efficiency.

2.3 The Hybrid Prototype (MAPv1.5)

The intermediate prototype, MAPv1.5, is a hybrid configuration with overall internal dimensions almost identical to MAPv1. As illustrated in Figure 3, the flashlamps remain integrated directly within the water-filled side panels. In these side panels, diffuse optical PTFE foil is utilized as the reflector material, as the alternative spectral silver reflectors cannot be placed directly inside the water to prevent corrosion effects.

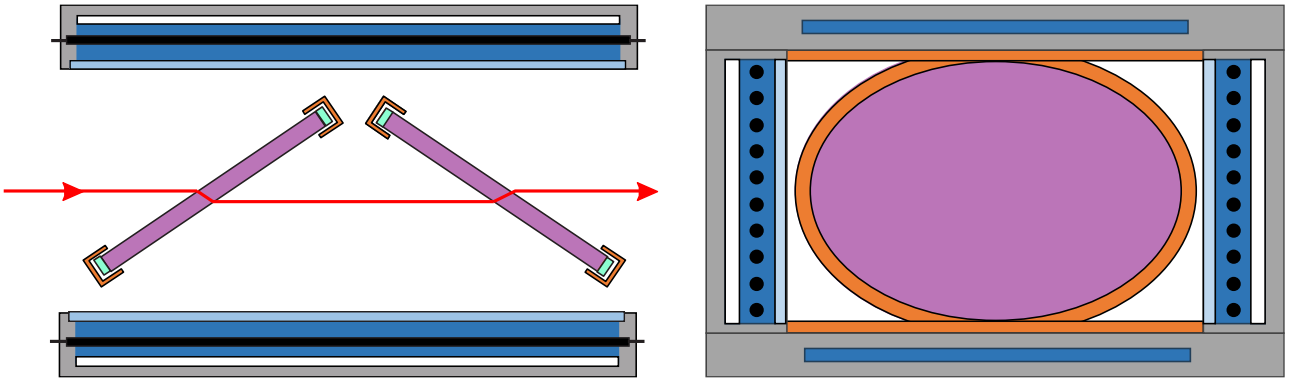


Figure 3: Schematic top-view (left) and front-view (right) cross-sections of the first hybrid amplifier prototype (MAPv1.5). The diagrams illustrate the laser axis (red arrow), housing (grey), silver reflectors (orange), optical PTFE reflectors (white with black frames), flashlamps (black), glass blast shields (light blue), cooling water volume (dark blue), Nd:glass slabs (purple), and edge cladding (cyan).

The primary structural modifications in MAPv1.5 concern the top and bottom panels and the slab mounts. The diffuse reflectors in the top and bottom sections were replaced with spectral silver

reflectors. These top and bottom silver reflectors are arranged so that they are cooled only from the outside by the water volume, eliminating the intervening glass windows and water layers that were present in the MAPv1 design. Additionally, the interior geometry was modified by embedding the slab holders directly into the top and bottom panels, which removes the free space between the Nd:glass slabs and the housing. Furthermore, the slab holders can be actively water-cooled. Because the holders are in direct physical contact with the edge cladding of the Nd:glass slabs, this configuration enables direct conductive cooling of the cladding itself.

2.4 The Optimized Prototype (MAPv2)

The third prototype, MAPv2, builds upon the structural modifications of MAPv1.5 while maintaining almost identical overall dimensions. It incorporates the top and bottom spectral silver reflectors and the embedded, water-cooled slab holders introduced in the previous iteration, thereby retaining the capacity to directly cool the edge cladding.

The fundamental structural difference in MAPv2 is the placement of the flashlamps and the side reflectors. As shown in Figure 4, the flashlamps are positioned physically beside the water panels rather than inside the water volume. Consequently, the water layer is spatially separated from the flashlamps and serves purely as a thermal isolation barrier between the flashlamp arrays and the central optical cavity. Because the side cavities surrounding the flashlamps are no longer water-filled, spectral silver reflectors are currently utilized behind the flashlamp arrays. However, for the final design, the use of diffuse reflectors adjacent to the flashlamps is not excluded. As demonstrated in *Metternich, M.*, et al. (2025), employing diffuse materials at these specific positions does not negatively impact the overall pumping performance. Furthermore, diffuse reflectors offer significant practical advantages, notably easier to manufacture and enhanced longevity due to their inherent corrosion resistance.

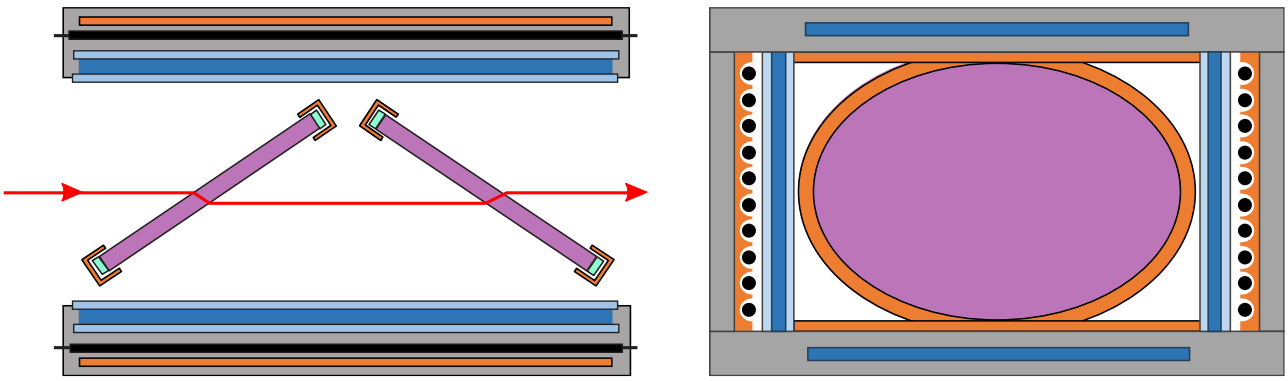


Figure 4: Schematic top-view (left) and front-view (right) cross-sections of the optimized main amplifier

prototype (MAPv2). The diagrams illustrate the laser axis (red arrow), housing (grey), silver reflectors (orange), optical PTFE reflectors (white with black frames), flashlamps (black), glass blast shields (light blue), cooling water volume (dark blue), Nd:glass slabs (purple), and edge cladding (cyan).

3 Prototype Characterization

This chapter presents the experimental characterization of the three main amplifier prototypes. Section 3.1 details the experimental methodology and the diagnostic setup utilized for the measurements. Section 3.2 analyzes the Nd:glass pumping efficiency, directly comparing the performance of the water-cooled prototypes to the conventional PMA. Finally, Section 3.3 discusses the thermal recovery and long-term aberration measurements.

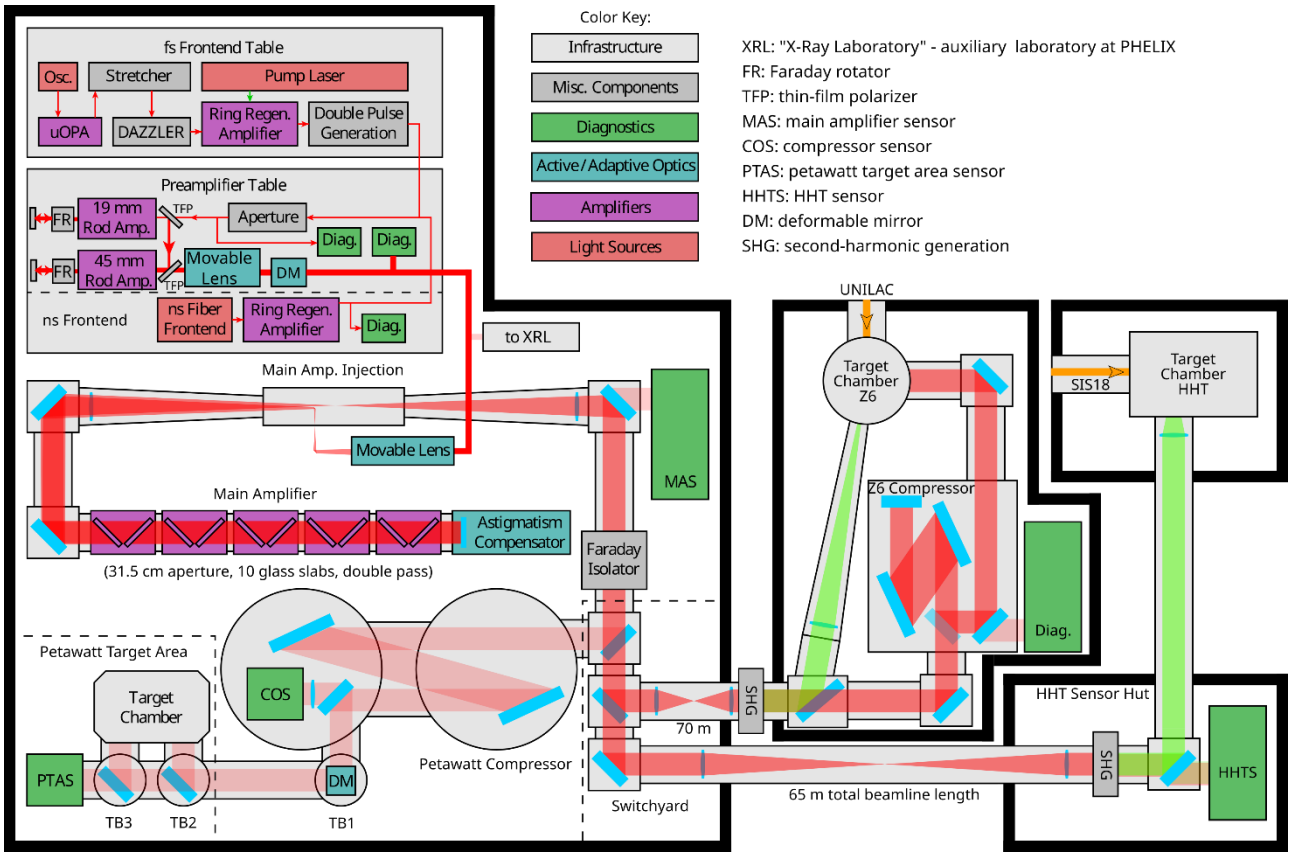


Figure 5: Schematic overview of the PHELIX laser system infrastructure. The diagram illustrates the chirped pulse amplification (CPA) architecture, highlighting the dual frontends (nsFE and fsFE), the preamplifier section featuring the 19 mm rod amplifier, the main amplifier chain, and the key diagnostic sensors, including the Main Amplifier Sensor (MAS) at the exit. The original version of this figure was created by Ohland, J. B..

3.1 Characterization Methodology

To evaluate the performance of the prototypes, the third conventional PHELIX main amplifier (PMA 3) in the main amplifier chain was exchanged with the respective prototype for the measurements. As illustrated in the system overview in Figure 5, PHELIX is a chirped pulse amplification (CPA) laser system equipped with two distinct frontends: a nanosecond frontend (nsFE) and a femtosecond frontend (fsFE).

Depending on the specific measurement series, pulses originating from these frontends were utilized as the active probe beam. To ensure clarity, the specific probe laser frontend used during a given measurement is consistently indicated in the legends of the respective data plots. Furthermore, a continuous-wave (cw) alignment laser is integrated into the beamline to facilitate preliminary alignment and system setup, and was also partially utilized as the probe beam for the long-term aberration measurements.

The optical performance was monitored using a comprehensive diagnostic suite. The diagnostic stations feature energy meters to record the pulse energy, near-field and far-field cameras to evaluate the spatial beam profile, and a Shack-Hartmann wavefront sensor (SHS) for precise wavefront measurements and aberration analysis.

3.2 Nd:glass pumping efficiency

To ensure that the probe beam possessed sufficient energy for accurate and reliable detection by the diagnostic equipment, it was first pre-amplified using the 19 mm rod amplifier of PHELIX. The gain was then determined by recording the pulse energy at two specific diagnostic points: the first energy meter is located at the exit of the preamplifier, serving as the input reference energy for the main amplifier stage, and the second energy meter is positioned at the Main Amplifier Sensor (MAS). To account for the passive transmission losses of the beamline, reference shots were recorded wherein the probe beam propagated through the system without discharging the flashlamps of the amplifier under test. By evaluating the energy ratio between the two diagnostic points and correcting for this baseline transmission, the active single-pass gain relative to the electrical input energy was determined.

These measured gain values were subsequently converted into the overall Nd:glass pumping efficiency to provide a direct, quantitative comparison between the different amplifier cavity designs. The pumping efficiency was defined as the ratio of the total stored optical energy in the upper laser level to the electrical input energy supplied by the capacitor banks. The stored energy was derived from the measured single-pass gain of the ns-frontend, assuming a homogeneously pumped gain

distribution across the active glass volume, excluding the highly absorbing edge cladding. This calculation utilized the effective stimulated emission cross-section of the Schott LG-750 Nd:glass (approximately 3.7×10^{-20} cm²) and the photon energy at the probe wavelength to determine the stored energy density. This density was then multiplied by the total pumped volume of the slabs to calculate the total stored energy, which was finally divided by the electrical input energy to yield the pumping efficiency.

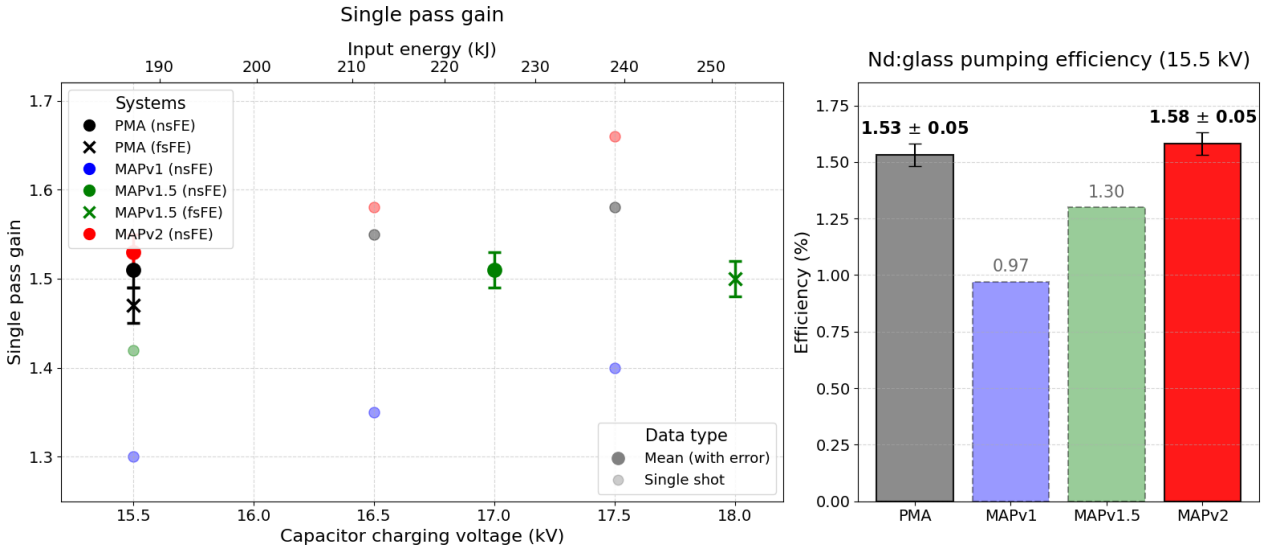


Figure 6: Single-pass gain as a function of the capacitor charging voltage and electrical input energy (left), alongside the corresponding calculated Nd:glass pumping efficiency at a standard charging voltage of 15.5 kV (right). The markers denote the specific frontend utilized as the probe laser (nsFE or fsFE) for the conventional PMA and the MAP prototypes. Opaque markers with error bars represent mean values and their standard deviations, whereas semi-transparent markers denote single-shot measurements.

Previous investigations of the first prototype (MAPv1) revealed a drastic drop in pumping efficiency compared to the conventional PMA. As confirmed by the recent measurement series (see Figure 6, right), the efficiency of MAPv1 at a standard capacitor charging voltage of 15.5 kV was merely 0.97%, whereas the conventional PMA achieved 1.53 ± 0.05%. This significant loss of nearly 30% was primarily attributed to four factors:

1. Direct absorption of the infrared pump light by the cooling water.
2. Total and Fresnel reflections at the water-glass-air interfaces, which trapped light within the side panels, increased the optical path in the water, and thereby amplified the absorption.
3. Increased reabsorption of pump light by the flashlamps. Because radiation was trapped within the side panels by total internal reflection at steep angles, a significant portion was redirected back into the flashlamp plasma. Although the flashlamps can recycle and re-emit this radiation, this conversion process involves inherent energy losses, meaning any light forced back into the

flashlamps ultimately reduces the total optical power reaching the gain medium.

4. An unfavorable geometry utilizing diffuse optical PTFE reflectors on the top and bottom, which partially redirected light back into the flashlamp panels instead of directly onto the Nd:glass slabs.

To verify these hypotheses and recover the lost efficiency, the modified prototypes MAPv1.5 and MAPv2 were characterized. Figure 6 (left) displays the single-pass gain as a function of the charging voltage and input energy, while Figure 6 (right) summarizes the calculated Nd:glass pumping efficiency at 15.5 kV. The measurement data fully validate the previously established hypotheses and demonstrate a successive performance increase driven by the targeted design changes.

The hybrid prototype MAPv1.5 achieved a significantly improved pumping efficiency of 1.30%. Although the flashlamps in this design remained directly submerged in the water of the side panels, the geometric modifications to the top and bottom alone yielded a substantial efficiency gain. Replacing the diffuse PTFE with spectral silver reflectors and embedding the slab holders directly into the panels confirmed the light-guiding hypothesis: the spectral reflector geometry prevents pump light from becoming trapped or backscattered to the flashlamp panels. Instead, the radiation is directed efficiently onto the Nd:glass slabs.

The optimized prototype MAPv2, in which the flashlamps were completely removed from the water and placed beside the water panels, demonstrates the decisive leap in performance. With an Nd:glass pumping efficiency of 1.58(5) %, MAPv2 clearly surpasses the hybrid intermediate stage and achieves a value slightly higher than the conventional PMA. This performance recovery is also reflected in the direct comparison of the single-pass gain, where MAPv2 at 15.5 kV ranks slightly above the conventional reference. It should be noted, however, that this minor performance surplus of MAPv2 over the PMAs could potentially be attributed to the use of newer flashlamps and pristine silver reflectors in the prototype assembly.

This result unequivocally proves the massive optical losses caused by the water in the original MAPv1 design. By spatially separating the flashlamps from the cooling water, total internal reflections at steep angles were eliminated, reducing both the optical path of the pump light through the water and the probability of radiation being reabsorbed by the flashlamp plasma.

In conclusion, the structural modifications in MAPv2 successfully resolve the efficiency drawbacks of the initial water-cooled design. The combination of targeted specular reflection, the prevention of pump light reabsorption by the flashlamp plasma, and the reduction of optical path length of light within the cooling water results in a pumping efficiency that is fully competitive with established, nitrogen-flushed systems.

3.3 Thermal Recovery

To fully contextualize the thermal performance of the water-cooled prototypes, it is necessary to briefly revisit the thermal management limitations of the PMAs. Pumping at standard energy levels generates a massive thermal load that is primarily removed via convective nitrogen gas flushing. Because the incoming gas transports waste heat from the flashlamp arrays directly into the central optical cavity, this structural flaw leads to severe thermal gradients in the interior of the amplifier. Overcoming the resulting 90-minute thermal recovery period was the primary driver for developing the water-cooled MAP series. It should be noted that the long-term aberration characterization campaigns for these prototypes were conducted during scheduled PHELIX maintenance periods. Consequently, the standard frontends (nsFE and fsFE) were not always available, necessitating the use of different probe lasers (including a continuous-wave alignment laser) across various measurement series.

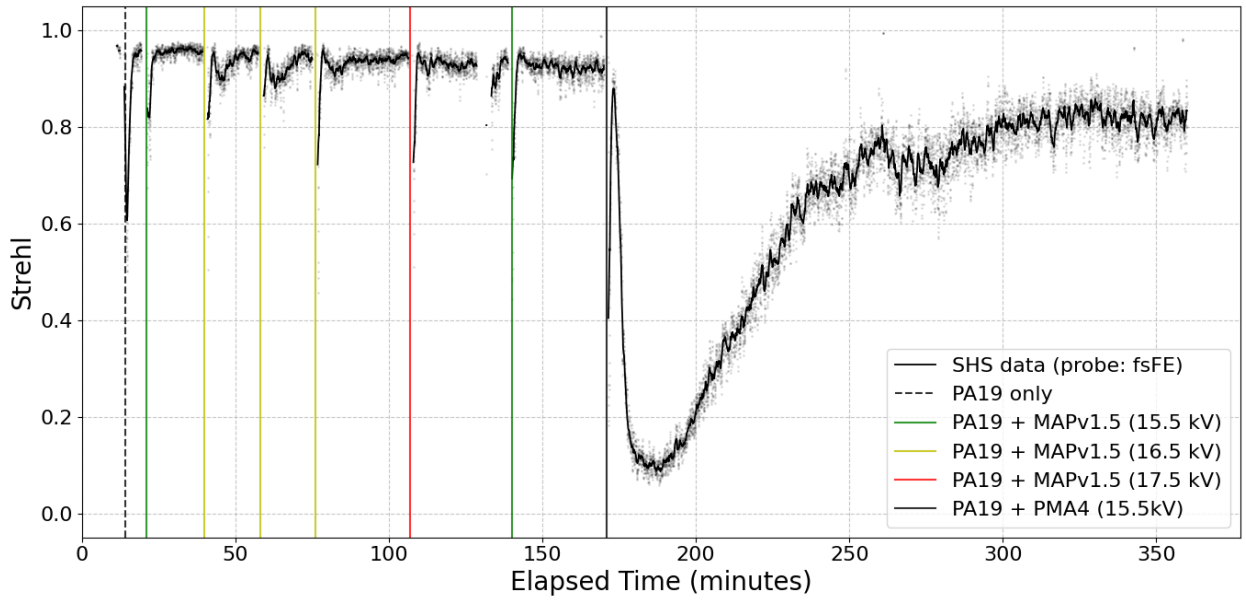


Figure 7: Strehl ratio evolution comparing several shots of the MAPv1.5 prototype to a single shot of the conventional PHELIX main amplifier (PMA4). The plot highlights the rapid recovery of MAPv1.5, the massive thermal bottleneck of PMA4, the sharp initial defocus caused by the preamplifier (PA19 only, dashed line), and a slight baseline drift in the Strehl ratio.

The wavefront measurement data unambiguously demonstrates the thermal superiority of the active liquid cooling approach. As depicted in Figure 7, the conventional PMA requires approximately 90 minutes to fully recover its initial Strehl ratio after a single full-energy shot. This initial measurement also highlights two general systemic behaviors. First, the 19 mm rod amplifier of PHELIX (PA19) introduces a strong defocus immediately following the shot, leading to a sharp initial drop in the

Strehl ratio; however, this effect decays rapidly within minutes and does not dictate the long-term recovery of the main amplifier chain. Second, over extended measurement windows, the baseline Strehl ratio sometimes settles around 0.80(5), failing to perfectly return to the pristine initial values of 0.9 or above. The exact cause of this incomplete baseline recovery requires further investigation. While it may be related to the repetitive firing of the amplifier, it is currently hypothesized to be a day-dependent effect caused by general ambient temperature drifts within the laser bay facility. This hypothesis is strongly supported by the observation that these residual aberrations do not decay on the typical 90-minute timescale of the conventional PMA, which would normally be expected if the distortions were driven by heat progressively accumulating within the amplifier cavity. An alternative hypothesis suggests that the Nd:glass slabs themselves gradually heat up directly from the optical pumping and subsequently cool down at a rate significantly slower than this 90-minute timescale. Nevertheless, the day-dependent ambient drift remains the most probable explanation for now.

Focusing on the hybrid prototype, MAPv1.5 demonstrates stable thermal recovery that supports significantly higher repetition rates. Figure 8 illustrates continuous shot series at 10-minute and 5-minute intervals. While both operational rates are fundamentally possible, the 5-minute interval naturally leads to a faster and more pronounced degradation of the Strehl ratio during the series, as the residual heat does not fully dissipate between shots. However, detailed wavefront analysis reveals that this degradation consists primarily of low-order aberrations, specifically defocus and astigmatism. For future high-energy, high-repetition-rate (HEHRR) upgrades, such predictable low-order distortions can likely be dynamically compensated using adaptive optics, making even these demanding shot rates highly viable.

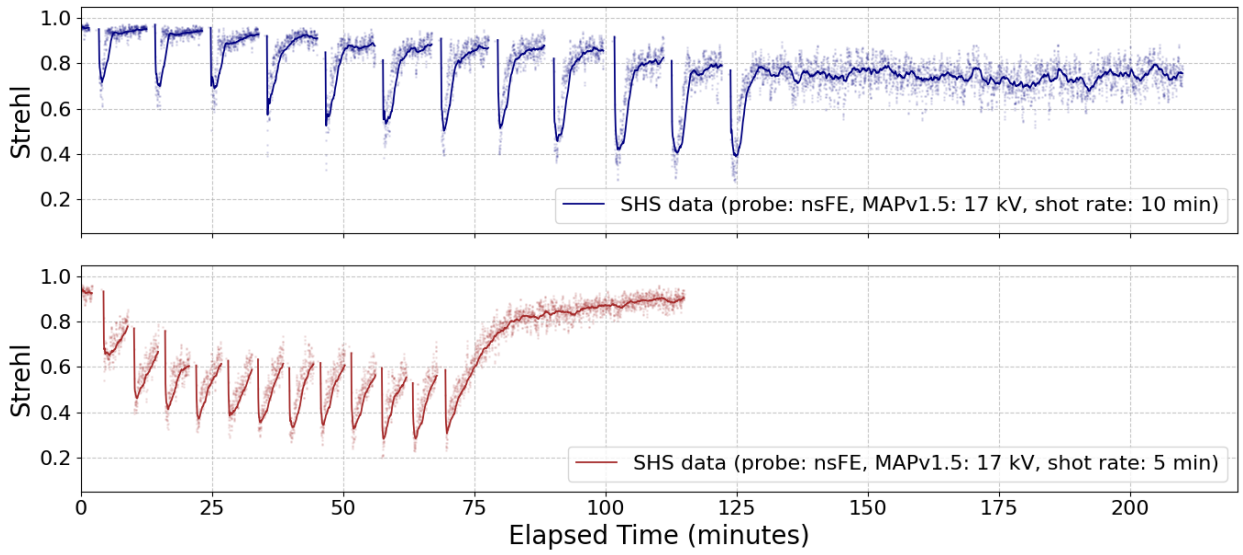


Figure 8: Strehl ratio measurements during continuous shot series for MAPv1.5 at 10-minute (top) and 5-minute (bottom) intervals. Higher repetition rates lead to a deeper cumulative Strehl drop, which is dominated by low-order aberrations as defocus and astigmatism.

Further investigations were conducted on MAPv1.5 to assess the impact of different water flow rates (e.g., 5 l/min vs. 10 l/min) and active edge-cladding cooling on overall thermal stabilization (see Figure 9). Interestingly, the data suggests that a baseline configuration utilizing a lower flow rate of 5 l/min without active cladding cooling appears to perform slightly better than configurations with higher flow rates or with cladding cooling. There are two primary hypotheses for this observation. First, higher water flow rates could induce increased turbulence and non-laminar flow patterns within the panels, which in turn could negatively impact the thermal isolation of the interior by the water. Second, regarding the active edge-cladding cooling, extracting heat exclusively from the slab's periphery may cool the overall volume, but in the short term, it actually steepens the radial temperature gradient from the outer edge to the warm center of the slab. This increased thermal gradient can temporarily exacerbate optical aberrations rather than mitigating them. However, the most likely overarching explanation is that these relatively minor discrepancies fall entirely within the margin of day-to-day environmental fluctuations. Regardless, the data provides no evidence that elevated flow rates or direct cladding cooling yield fundamentally superior thermal stability.

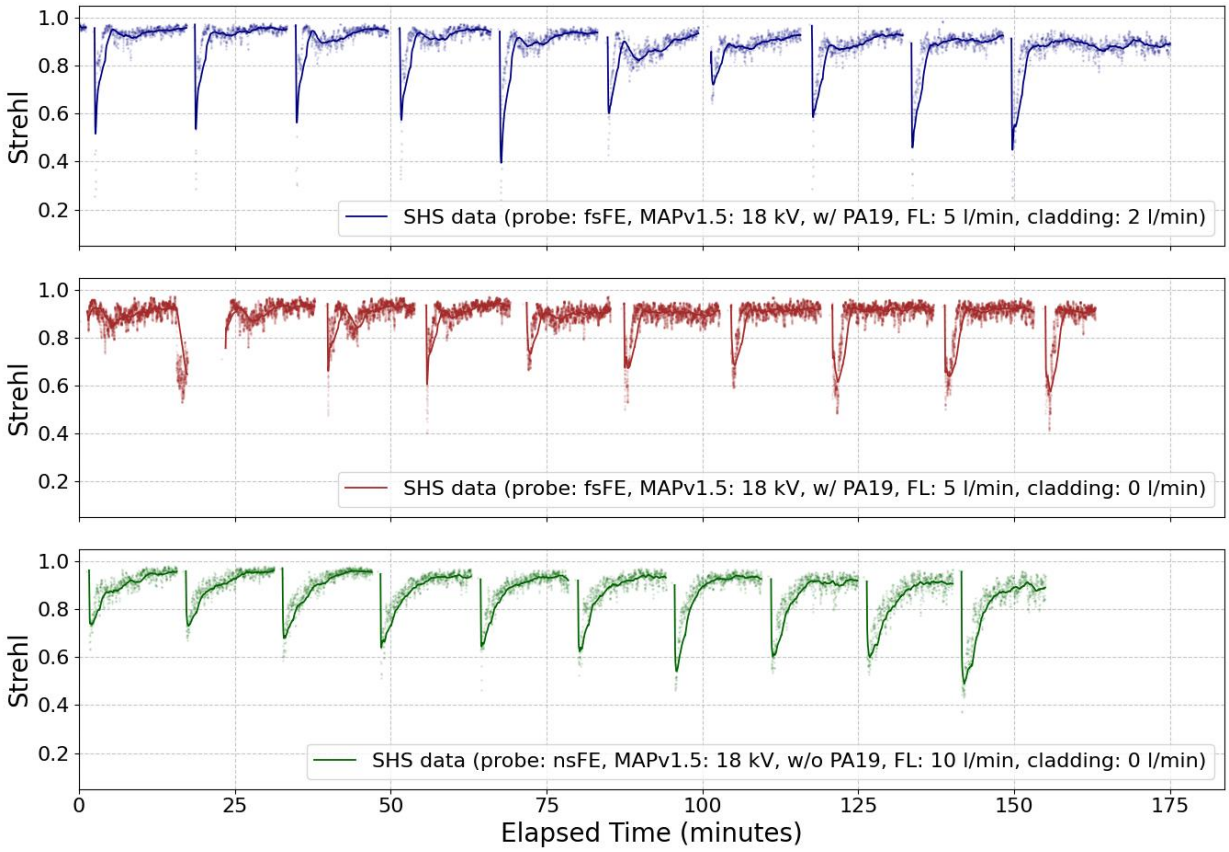


Figure 9: Thermal recovery profiles of MAPv1.5 under varying cooling parameters, including different water flow rates and cladding cooling settings. The nearly identical curves demonstrate no significant dependency on exact flow adjustments, with lower flow rates performing comparably well or slightly better.

A direct comparison between the two latest iterations, MAPv1.5 and MAPv2, reveals very similar, rapid recovery dynamics. As shown Figure 10, both prototypes exhibit robust recovery to a Strehl ratio of approximately 0.90 at a conservative 15-minute shot interval. There is no evidence to suggest that the optimized geometry of MAPv2 prolongs the thermal recovery time compared to MAPv1.5. Despite the minor astigmatic features expected from the aforementioned low-order aberrations, the overall spatial beam quality remains excellent, as qualitatively evidenced by the highly stable focal spot profiles recorded throughout the MAPv2 shot series (see Figure 11).

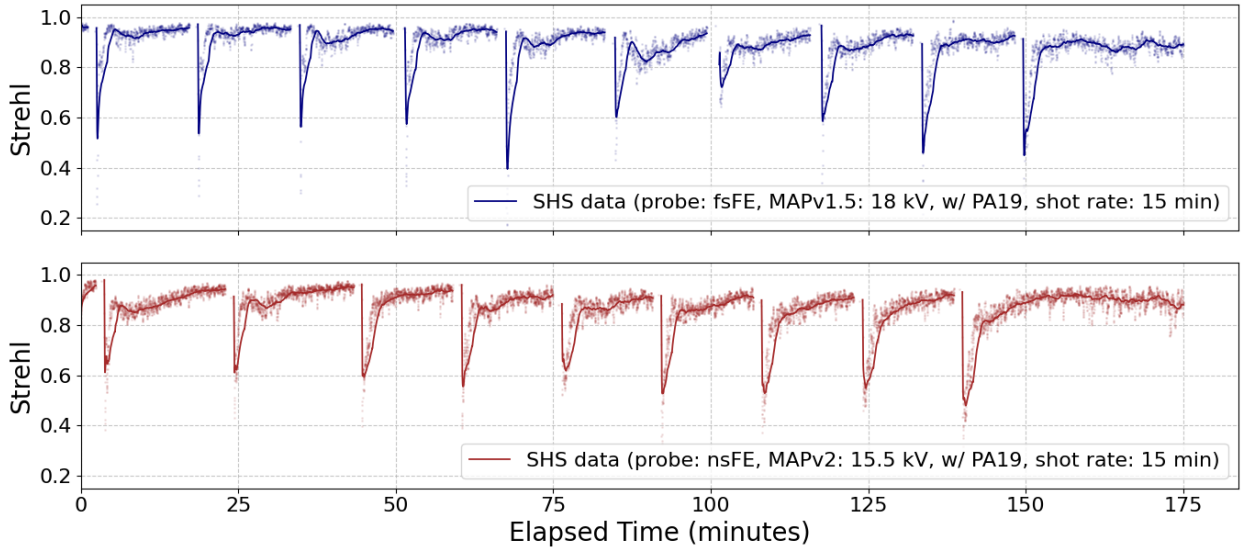


Figure 10: Comparison of the Strehl ratio recovery during a 15-minute shot series for MAPv1.5 and MAPv2, showing comparable thermal stabilization capabilities.

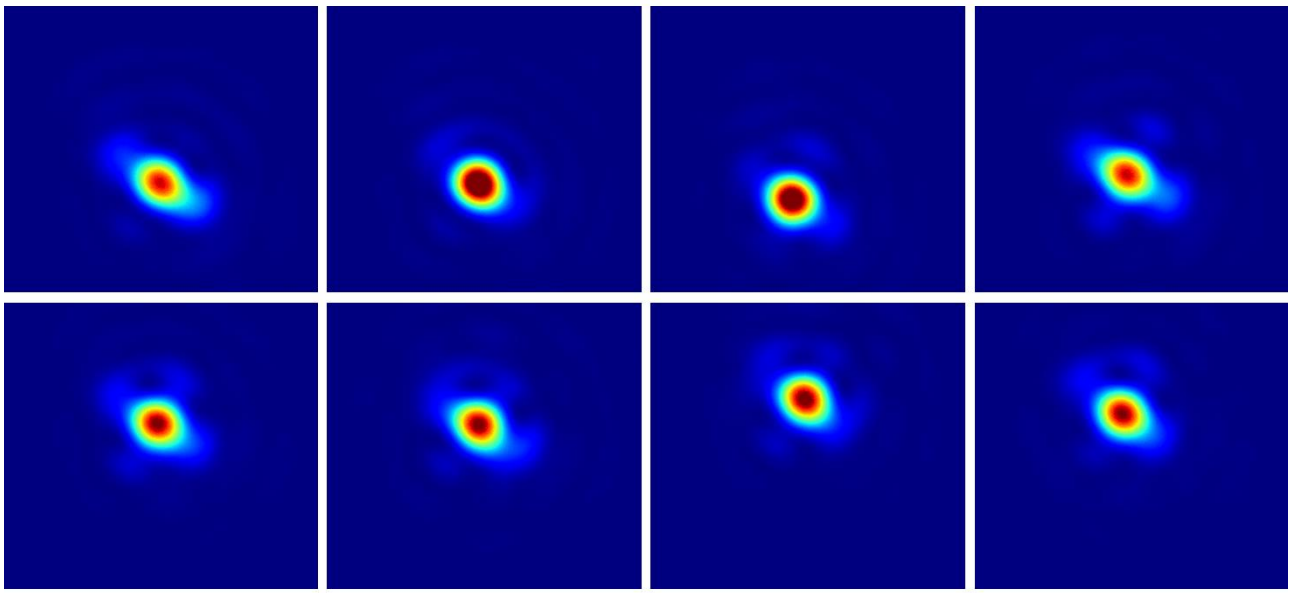


Figure 11: Focal spot profiles recorded during a MAPv2 shot series (lower measurement from Figure 10) using the nsFE probe laser, demonstrating stable spatial beam quality.

4 Conclusion and Outlook

The primary objective of this investigation, conducted within WP4 of the European THRILL project, was to test alternative schemes for high-energy, high-repetition-rate amplifiers that resolves the severe thermal bottlenecks of conventional nitrogen-flushed systems without sacrificing Nd:glass pumping efficiency. The optimized prototype, MAPv2, successfully fulfills all of these criteria.

By relocating the flashlamps outside the water panels and utilizing an optimized spectral silver reflector cavity, MAPv2 completely eliminates the parasitic water absorption and total internal reflection issues that heavily degraded the efficiency of the first prototype (MAPv1). As a result, MAPv2 perfectly matches the pumping efficiency of the conventional PHELIX main amplifiers, while simultaneously reducing the mandatory thermal recovery time between shots from 90 minutes to under 15 minutes.

Beyond fully achieving the targeted optical and thermal performance, the structural design of MAPv2 offers three decisive practical and technical advantages over the hybrid MAPv1.5 iteration:

- **Reduced Capital Costs and Footprint:** Because the flashlamps are no longer directly submerged in the cooling liquid, the immense waste heat generated by the flashlamp plasma is not entirely absorbed by the water. This drastically reduces the peak heat load on the external chiller system. Consequently, the required cooling capacity is significantly lower, which translates to a substantial reduction in both the upfront capital investment and the physical space needed for the chiller infrastructure.
- **Enhanced Maintenance and Cleanliness:** If a flashlamp fails or requires replacement, the external flashlamp panels can be removed without breaching the central optical cavity. Because the interior remains completely sealed off by the glass water panels, no dirt, debris, or moisture can contaminate the delicate Nd:glass slabs during maintenance.
- **Reduced Pulsed Power Stress:** MAPv2 efficiently provides the necessary single-pass gain for PHELIX operations at a highly moderate capacitor charging voltage of 15.5 kV. This prevents the need to overdrive the system, minimizing the electrical stress on the pulsed power infrastructure and ensuring exceptional component longevity.

Given these optical, thermal, and operational advantages, MAPv2 has proven to be the overall superior design. It successfully bridges the gap between high pumping efficiency and high repetition rates, and will consequently serve as the architectural baseline for future upgrades to the PHELIX main amplifier chain for which the financing is currently close to approval and should happen in the

coming years.

Although the approach of actively cooling the laser glass is not yet included in the currently proposed amplifier head design, the development will likely be continued beyond the THRILL project because several issues still have to be addressed for future laser system designs. For example, the transmitted wavefront measured with the uncooled laser glass so far has proven to recover after about 10 minutes for a single laser head with an acceptable amount low-order aberrations, but it cannot be excluded yet that a system of five or more heads in series will suffer from heat buildup in the laser glass, resulting in a combined wavefront deterioration which so far could not be detected or might not be easy to compensate. And although the remaining low-order aberrations are easier to compensate than high-order structures, robust measurement and compensation schemes, able to deal with irregular shot sequences as opposed to strictly periodic ones, remain challenging, even though some of these were already addressed in THRILL WP 5.2 which will continue in the recently established Young Investigator Group Project ALADIN. Along similar lines, the thermal load on the absorptive cladding attached to the slabs' edges will increase with the higher repetition rate and mitigation is expected become necessary to ensure the system's performance at elevated repetition rates in the long run.

5 References

Metternich, M., Reemts, D., Brabetz, C., Lehmann, D., Quandt, A., Zielbauer, B, Bagnoud, V. (2025). The influence of flashlamp water cooling in long-term aberrations in large aperture Nd:glass amplifiers. Proc. SPIE 13535, Research Using Extreme LIGHT Infrastructures; New Frontiers with Petawatt-Level Lasers VI, 1353509; DOI: https://doi.org/10.1117/12.3058409.

Ohland, J. B., *Design and setup of a post-compressor adaptive optics loop at PHELIX.* (2022). Ph.D. Thesis, TU Darmstadt; DOI: 10.26083/tuprints-00021995